2. Symko, O. G., Abdel-Rahman, E., Kwon, Y. S., Emmi, M., and Behunin, R., 2004, Design and development of high-frequency thermoacoustic engines for thermal management in microelectronics, Microelectronics Journal, **35**, pp. 185-191.
3. Duffourd, S., 2001, Réfrigérateur thermoacoustique: études analytiques et expérimentales en vue d'une miniaturisation, PhD thesis, ECL 2001-06, Ecole Centrale de Lyon.
4. Worlikar, 1997, A., Numerical simulation of thermoacoustic refrigerator, PhD thesis, The Johns Hopkins University, Baltimore.
5. Waxler, R., 2001, Stationary velocity and pressure gradients in a thermoacoustic stack, J. Acoust. Soc. Am., **109**, 2739--2750.
6. Bailliet, H. A., Gusev, V., Raspet, R., and Hiller, R. A., 2001, Acoustic streaming in closed thermoacoustic devices", J. Acoust. Soc. Am., **110**, pp. 1808–-1821.
7. Hamilton, M. F., Ilinskii, Y. A., and Zabolotskaya, E. A., 2003, Acoustic streaming generated by standing waves in two-dimensional channels of arbitrary width, J. Acoust. Soc. Am., **113**,pp. 153–-160 .
8. Poese, M. E., and Garrett, S. L., 2000, Performance measurements on a thermoacoustic refrigerator driven at high amplitudes, J. Acous. Soc. Am., **107**, pp. 2480-2486.
9. Cao, N., Olson, J., Swift, G. W., and Chen, S., 1996, Energy flux density in a thermoacoustic couple, J. Acoust. Soc. Am., **99**, pp. 3456-3464.
10. Marx, D., and Blanc-Benon, Ph., 2004, Numerical simulation of the stack-heat exchangers coupling in a thermoacoustic refrigerator. AIAA Journal, **42**, pp.1338-1347.
11. Marx, D., 2003, Simulation numérique d'un réfrigérateur thermoacoustique, PhD Thesis, ECL 2003-34, Ecole Centrale de Lyon.
12. Gusev, V., Lotton, P., Bailliet, H., Job, S., and Bruneau, M., 2001, Thermal wave harmonics generation in the hydrodynamical heat transport in thermoacoustics, J. Acous. Soc. Am., **109**, pp. 84-90.
13. Besnoin, E., Numerical study of heat exchangers, 2001, PhD Thesis, The Johns Hopkins University, Baltimore.
14. Blanc-Benon, Ph., Besnoin, E., and Knio, O., 2003, Experimental and computational visualization of the flow field in a thermoacoustic stack, C. R. Mecanique, **331**, pp. 17-24.
15. Bogey, C. and Bailly, C., 2004, A family of low dispersive and low dissipative explicit schemes for flow and noise computations, J. Comput. Phys., **194**, pp. 194--214.

G.Penelet[1], V.Gusev[1,2], P.Lotton[1], and M.Bruneau[1]

EXPERIMENTAL AND THEORETICAL STUDIES OF NONLINEAR SATURATION PROCESSES IN ANNULAR THERMOACOUSTIC PRIME MOVERS

[1]Laboratoire d'Acoustique de l'Universite du Maine, UMR CNRS 6613
[2]Laboratoire de Physique de l'Etat Condensé, UMR CNRS 5509
Avenue Olivier Messiaen, 72085 Le Mans Cedex 9, France
Phone : (33) 243 83 36 26, Fax : (33) 243 83 35 20
E-mail : guillaume.penelet@univ-lemans.fr

The present study gives a simplified analytical description of spontaneous generation and finite amplitude saturation of sound in annular thermoacoustic engines, and also provides comparison with experiments. The model includes the description of thermoacoustic amplification of sound (induced by interaction between an heterogeneously heated stack of solid plates and resonant gas oscillations), which accounts for the details of the temperature distribution in the whole thermoacoustic device. The saturation of the acoustic wave amplitude is described by taking into account both the reverse influence of the acoustic field on the temperature field, and the dissipation of acoustic power due to

higher harmonics generation and minor losses (vortex generation). From the comparison between simulation results and experiments, it is demonstrated that the dynamical behavior observed in our experimental device is predominantly controlled by the effects of acoustic streaming and acoustically enhanced thermal conductivity tending not only to reduce the externally imposed temperature gradient along the stack, but also to change the shape of the temperature field in such a way that additional thermoacoustic amplification may occur.

1. Introduction

Thermal interactions between solid walls and oscillating gas are responsible for various thermoacoustic phenomena such as self sustained acoustic waves in resonators or acoustic heat pumping. Since the early 80's, there has been a renewal of interest in thermoacoustic devices, both prime movers (i.e. thermal to acoustic energy converters) and heat pumps, so that a great variety of devices has been developed. The linear analytical theory of thermoacoustics is now well developed [1], but not sufficient to understand the great complexity of such heat engines. In particular, it is now well established that steady-state sound in thermoacoustic prime movers is controlled by a few nonlinear effects, but it is however difficult both to predict the acoustic pressure amplitude in the steady regime and to clearly understand the processes controlling the dynamics of wave amplitude evolution observed experimentally, even in very simple thermoacoustic devices. The role of the cascade process of higher harmonics excitation has been studied both experimentally [2] and theoretically [3,4], and the minor losses due to vortex generation at the edges of the stack and of the heat exchangers has been estimated [5]. In addition to these classical saturation processes, the nonlinear processes involving the reverse influence of the acoustic waves on temperature distribution have been observed [6,7]. Among these mechanisms is the well-known effect of thermoacoustic heat transport from hot to cold ends of the stack induced by gas oscillations [6] which tends to reduce the externally imposed temperature gradient. Another mechanism is the excitation of acoustic streaming, i.e. the acoustically induced generation of a mean (non oscillating) mass flow, which influences the temperature distribution in the device. Though an important research effort has recently been devoted to the description of acoustic streaming in resonant tubes [8,9]and thermoacoustic devices [10,11], the role of this mechanism in thermoacoustic prime movers is poorly understood : its presence has been evidenced in various thermoacoustic devices, but the physics of its influence on the saturation of the wave amplitude growth in the prime movers have not yet been completely explained.

We failed to find in the literature any (necessarily simplified) analytical description of the transient regime which accounts for all the above mentioned nonlinear processes and which agrees reasonably well with experimental results. Thus, the present study was initiated to reach a better understanding of the acoustic wave saturation in thermoacoustic devices, and to propose a model able

to reproduce, at least qualitatively, the typical dynamic behaviors observed in particular thermoacoustic devices.

2. Experimental apparatus, experiments.

The thermoacoustic device which is studied here is presented schematically in Fig. 1 (a): this is an annular thermoacoustic prime mover. It is basically composed of a resonant annular tube and a stack of solid plates submitted to a strong temperature gradient. The torus-shaped stainless steel tube of length L=2.24 m is filled with air at atmospheric pressure $p_0 \approx 10^5$ Pa. The stack (length H_S=5 cm) is a honeycombed ceramic material with square channels of cross-section 0.9×0.9 mm^2. The cold heat exchanger consists of a copper circular shell set around the tube with flowing cooling water inside at room temperature T_∞, and a copper wire mesh in the tube (attached to the left side of the stack). In order to impose a strong temperature gradient along the stack, two different heating processes have been used. The first one, which we call "internal heating" (see Fig. 1(b)), proceeds using a honeycombed ceramic material placed inside the waveguide 5 mm away from the right side of stack, and used as a skeleton for the coiling of a nichrome wire (i.e. an electrical heat resistance) connected to a thyristor unit. The second one, called "external heating", proceeds using eight electrical heat resistances soldered in a stainless steel block set at the right side of stack around the outer perimeter of the tube (Fig. 1(c)).

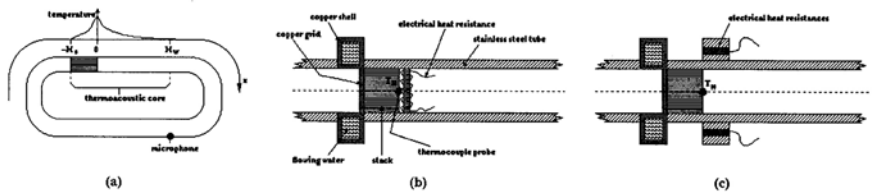

Fig. 1. (a) Schematic representation of the experimental apparatus. (b) Detailed representation of the thermoacoustic core in case of "internal heating". (c) Detailed representation of the thermoacoustic core in case of "external heating".

In such a device, when the temperature gradient along the stack exceeds a certain critical value, the thermoacoustic amplification process (which occurs in the stack, inside thermal boundary layers) results in the self excitation of high amplitude resonant acoustic waves. This is called the onset of thermoacoustic instability. For each of the measurements presented in the following, the heating power supply is preliminarily set to Q_0 so that the device is just below the onset of thermoacoustic instability. A small ΔQ increment is then sufficient for the acoustic wave to be generated in the waveguide at frequency f≈153 Hz, which corresponds approximately to the frequency of the first travelling wave mode of the annular resonator (f≈c/L, where c≈340 m.s^{-1} denotes the adiabatic sound velocity). It is schematically shown in Figs. 1(b-c) that the temperature T_H at the hot stack end is measured using a type K thermocouple probe glued with a

ceramic putty onto the stack. The amplitude of acoustic pressure oscillations p_1 is measured using a piezoresistive microphone placed approximately 1 metre away from the hot stack end. Note that subscript "1" is used in this paper as a reminder that acoustic pressure is a quantity of the first order of smallness in comparison with static pressure ($p_1 << p_0$).

Figures 2 and 3 present the observed dynamics of the transient regime for various ΔQ increments on the heating power supply above the threshold value Q_0, in cases of external heating (Fig. 2) and internal heating (Fig. 3), respectively. It is remarkable here that the dynamics of wave amplitude growth strongly depends on the stack heating process. While in case of external heating, the onset of thermoacoustic instability results in the exponential growth of the acoustic pressure amplitude, followed by a regime of stabilization, the results also show, in case of internal heating, the possibility for the device to turn on and off spontaneously and periodically and the switch on/off period decreases when ΔQ increases. Furthermore, additional information is provided by the analysis of temperature T_H.

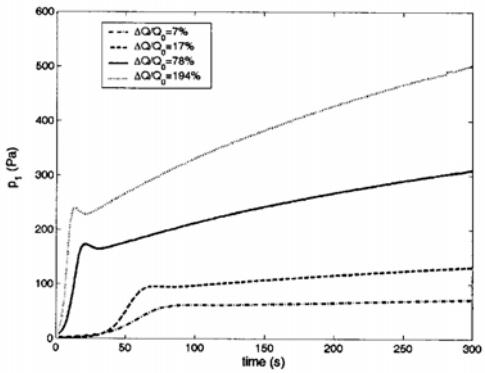

Fig. 2. Gradual evolution of the root mean square amplitude p_1 of acoustic pressure, for various ΔQ increments of the heating power supply above the critical value Q_0, in case of external heating.

First of all, while in the case of internal heating the temperature T_H at threshold (with a corresponding $Q_0 \approx 55$ W) is of about 350°C (see Fig. 3, dashed lines), the onset occurs in the case of external heating as soon as T_H only exceeds 150°C (but with $Q_0 \approx 150$ W). Secondly, it is remarkable in Fig. 3 that the variations with time of T_H are strongly coupled to those of p_1: for small ΔQ increments(Fig. 3 (a-c)), periodic evolution of T_H is observed, while for larger ΔQ the stabilization of acoustic pressure amplitude is accompanied by the stabilization of T_H (Fig. 3(d)). It is also remarkable in Fig. 3(d) that the temperature T_H before the first onset of thermoacoustic instability (occuring at time $t \approx 0$ in Fig. 3(d)) is more than 30 degrees higher than its value when steady-state sound is obtained. From all of

these observations, it is concluded firstly that the thermoacoustic amplification process (and in particular the threshold condition) does not only depend on the temperature difference between stack ends, but also strongly on the shape of the temperature field in the entire heterogeneously heated part of the device [12], and secondly the results indicate that the nonlinear effects involving the reverse influence of the acoustic field on the temperature field may play the predominant role in the dynamics of prime mover operation.

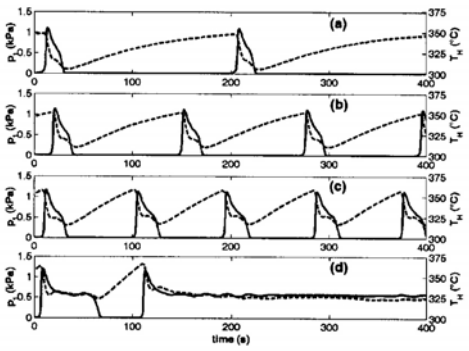

Fig. 3. Gradual evolution of p_1 (solid line) and T_H (dashed line), when the power increment ΔQ above the threshold value Q_0 is increased, in case of internal heating. (a) $\Delta Q/Q_0$=5%, (b) 10%, (c) 20%, (d) 30%.

3. Analytical model

The time-dependent regime of the prime mover operation is modelled here by combining the equation describing the variations of acoustic pressure amplitude with the equations describing, in a simplified one dimensional approach, the heat transfer through the heterogeneously heated parts of the device (which will be called "thermoacoustic core" in the remaining of the paper). Only the general outlines of the model are presented here, because the complete analytical approach can be found in previous papers [12,13]. Heat transfer throughout the thermoacoustic core is described by the coupling between three homogeneous media, which are the stainless steel resonator walls (with the corresponding temperature field $T_r(x,t)$), the air in the heterogeneously heated part of the waveguide ($T_w(x,t)$), and the stack (composed both of air and ceramics, but considered as a homogeneous medium at temperature $T_s(x,t)$ in the heat transfer equations). For example, in the case of internal heating, this results in the following set of equations:

$$x \in [-H_S, 0],\ \partial_t T_r = \kappa_r \partial^2_{xx} T_r - \gamma^{r\to s}(T_r - T_s) - \gamma^{r\to\infty}(T_r - T_\infty), \quad (1a)$$

$$x \in [-H_S, 0],\ \partial_t T_s + v_s \partial_x T_s = \kappa_s \partial^2_{xx} T_s - \gamma^{s\to r}(T_s - T_r), \quad (1b)$$

$$x \in [0, H_W],\ \partial_t T_r = \kappa_r \partial^2_{xx} T_r - \gamma^{r\to w}(T_r - T_w) - \gamma^{r\to\infty}(T_r - T_\infty), \quad (1c)$$

$$x \in [0, H_W],\ \partial_t T_w + v_w \partial_x T_w = \kappa_w \partial^2_{xx} T_w - \gamma^{w\to r}(T_w - T_r), \qquad (1d)$$

where ∂_t and ∂_x respectively stand for partial time and space derivative, and where $\kappa_{r,s,w}$ denote thermal diffusivities of the media. Several points need to be explained concerning Eqs. (1).

First of all, the coupling coefficients $\gamma^{r\leftrightarrow s,\ r\leftrightarrow w,\ r\to\infty}$ are approximate phenomenological coefficients obtained from heat transfer theory [14]. The calculation details leading to the analytical expressions for these coefficients can be found in ref. [13].

Secondly, the advection terms $v_{s,w}\partial_x T_{s,w}$ in Eqs. (1b,d) account for the effect of acoustic streaming, the mean flow velocities $v_{s,w}$ being controlled by the acoustic pressure amplitude. It should be mentioned that equating the effect of acoustic streaming with a unidirectional mass flow is an approximation, because the actual velocity distribution is much more complex (in particular there are upward and downward streaming currents across the duct). However, it is well established that in annular thermoacoustic prime movers (and in other thermoacoustic devices where a closed loop path exists) there is a mean nonzero mass flow through the duct (directed clockwise in Fig. 1(a)), which is supposed here to provide the most important share of convective heat transfer. From previous theoretical [10] and experimental works [15], it is then possible to derive a simplified analytical expression for the velocity of acoustic streaming [13]:

$$d_t v_{s,w} + \frac{v_{s,w}}{\tau_v} = \frac{\Gamma_v^{s,w}}{\tau_v} p_1^2, \qquad (2)$$

where it is proportional to the square of acoustic pressure amplitude, taking into account a delay τ_v in its onset.

Thirdly, another effect involving the reverse influence of the acoustic field on the temperature field is hidden in Eq. (1b). This is the well-known thermoacoustic enthalpy flow induced by gas oscillations [1,6], which tends to reduce the temperature gradient. This nonlinear effect is equivalent to an acoustically enhanced thermal conductivity [3,6] of the gas in the vicinity of the solid surfaces, so that in Eq. (1b), the thermal diffusivity κ_s is actually separated into a static component κ_{s0} (i.e. without acoustic oscillations) and a dynamic one as follows:

$$\kappa_s = \kappa_{s_0} + \Gamma_\kappa p_1^2. \qquad (3)$$

In addition to Eqs. (1) describing heat balance in the thermoacoustic core, constant temperature T_∞ at the edges of the thermoacoustic core ($x=-H_S$ and H_W) is considered. Also, in case of internal heating, the heat power supply Q is included in the equation describing continuity of heat flux at the stack/air interface (at x=0), while in case of external heating, it is included as an additional term in Eq. (1c) (see ref. [13] for further details).

In addition to the effects involving the reverse influence of the acoustic field on the temperature field, the saturation of the acoustic wave may also occur as a consequence of more usual nonlinear effects such as higher harmonics generation and minor losses. Both processes can be included as dissipation processes in the following set of equations describing the evolution of acoustic pressure amplitude [13]:

$$d_t p_1 = \Omega_{\text{ampl}} p_1 - \Omega_{\text{casc}} p_1 p_2 - \Omega_{\text{minor}} p_1^2, \qquad (4a)$$

$$d_t p_2 = \Omega_{\text{casc}} p_1^2 - \Omega_{\text{diss}} p_2, \qquad (4b)$$

where p_2 corresponds to the second harmonic component of acoustic pressure oscillations ($p_2 << p_1$) generated by usual nonlinear effects [16]. The first equation describes thermoacoustic amplification of the fundamental component of acoustic pressure ($\Omega_{\text{ampl}}\ p_1$), energy transfer from the fundamental wave to second harmonic ($-\Omega_{\text{casc}}\ p_1 p_2$), and dissipation of energy due to vortex generation at the edges of the stack ($-\Omega_{\text{minor}}\ p_1^2$).The second equation (Eq. (4b)) describes both the generation of second harmonic ($\Omega_{\text{casc}}\ p_1^2$) and its dissipation in the acoustic boundary layers ($-\Omega_{\text{diss}}\ p_2$). Importantly, it should be mentioned that the value of the amplification parameter Ω_{ampl} depends on the temperature distribution $T_{S,W}$ in the entire thermoacoustic core [12].

So, while Eqs. (1) are coupled to Eqs. (4) through the effects of acoustic streaming and acoustically enhanced thermal diffusivity, Eqs. (4) are coupled to Eqs. (1) through parameter $\Omega_{\text{ampl}}\{T_{S,W}\}$. Then, the spontaneous generation and saturation of sound in the annular thermoacoustic prime mover can be computed, using classical finite difference methods to solve the above listed set of nonlinear differential equations. Further details concerning the solving process, the values for geometrical and thermophysical properties of materials, and the estimates for the nonlinear parameters ($\Gamma_{v,\kappa}$, $\Omega_{\text{casc,minor,diss}}$, τ_v) can be found in ref. [13], while the method used to obtain $\Omega_{\text{ampl}}\{T_{S,W}\}$ is presented in ref. [12].

4. Results, discussion.

In the simulation results presented below, the protocol is analogous to the one used in experiments: the heating power is initially set to a fixed value Q_0 in order for the system to be just below threshold after computing the associated temperature field, and various ΔQ increments are then applied so that the onset occurs. Figure 4 presents the results obtained in case of external heating while Fig. 5 presents the results obtained in case of internal heating. Both Figs. 4 and 5 can be compared to Figs. 2 and 3, respectively.

From the comparison between experimental and theoretical results in both cases of heating geometry, and considering the numerous approximations made in the model, it is remarkable that calculations reproduce quite well (i.e. at least qualitatively) the dynamics observed in experiments. In case of external

heating, both the dynamical behavior of wave amplitude growth and the steady-state pressure levels obtained match experiments. In case of internal heating, both the periodic onset/damping of thermoacoustic instability for small $\Delta Q/Q_0$ and the stabilization of acoustic pressure to a finite value for larger $\Delta Q/Q_0$ are reproduced by the model. The observation that simulations match experiments in case of external heating while only qualitative agreement is obtained in case of internal heating may be attributed to the one dimensional approach in the description of heat transfer. Such an approach is indeed valid if the radial temperature distribution remains close to uniform : this is the case when the temperature

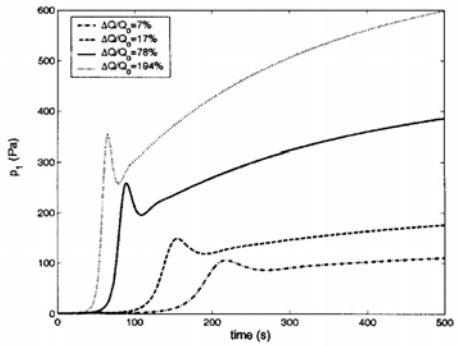

Fig. 4. Calculated evolution of p_1 for various ΔQ increments of the heating power supply above the critical value Q_0, in case of external heating.

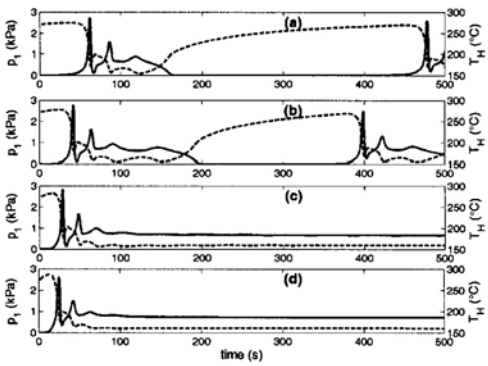

Fig. 5. Calculated evolution of p_1 (solid line) and T_H (dashed line), when the power increment ΔQ above the threshold value Q_0 is increased, in case of internal heating. (a) $\Delta Q/Q_0$=5%, (b) 10%, (c) 20%, (d) 30%.

gradient along the stack is imposed by heating the stainless steel resonator walls (Fig. 1 (c)) of high thermal inertia, while in case of internal heating (Fig. 1 (b)), a temperature difference of more than 100 K has been measured (just below

threshold) between the temperature T_H and the temperature at same position x=0 but 2 cm away from the stack's median axis.

Once it is clear that these results must be considered as qualitative ones, they however provide the opportunity to give a physical explanation of the observed dynamics, and in particular, deeper understanding can be reached from the analysis of the time dependent temperature field in case of internal heating.

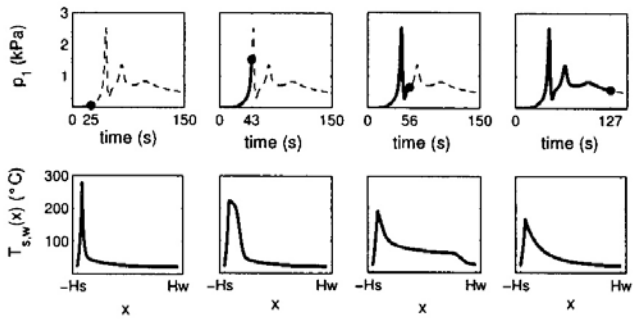

Fig 6 : Distributions of the temperature field $T_{S,W}(x)$ (bottom) corresponding to different moments (marked with •) the transient regime (top), obtained for ΔQ/Q0= 10% in case of internal heating

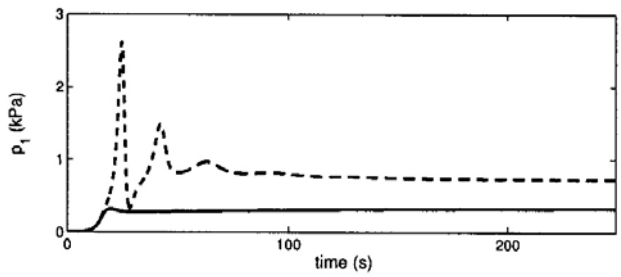

Fig 7 : Calculated evolutions with time of acoustic pressure amplitude p_1 when ΔQ/Q0= 30% (internal heating), whether the effect of acoustic streaming is included in the model (dashed line) or not (solid line).

Figure 6 presents different temperature distributions corresponding to different stages of the wave amplitude evolution, calculated for $\Delta Q/Q_0$=10% in case of internal heating. From the comparison of the temperature field $T_{S,W}(x,t=25s)$, corresponding to the beginning of the onset, to the temperature field $T_{S,W}(x,t=43s)$, it appears that while acoustic pressure strongly increases at time t=43 s, the hot temperature T_H has already dramatically decreased. The only way to explain such results is that the excitation of acoustic streaming has changed the shape of the temperature field in such a way that additional thermoacoustic amplification has occurred. This may well be the most important thing to understand from the analysis of Fig. 6, because it means that acoustic streaming

does not necessarily lower the engine's efficiency. Indeed, as illustrated in Fig. 7 which presents the results obtained when the effect of acoustic streaming is ignored in the model (solid line) compared to the case when it is included in the model (dashed line), it appears that the acoustic pressure amplitude in the steady regime is twice as high with than without account of acoustic streaming. So, an important, very practical conclusion of the results presented in this paper is that acoustic streaming may, in theory, play a favorable role if it contributes to tune the shape of the temperature field throughout the heterogeneously heated parts of the device in such a way that thermoacoustic amplification in the stack is optimized.

REFERENCES

1. Rott N. Thermoacoustics // Adv. Appl. Mech. 1980, V.20, P. 135.
2. Swift G.W. Analysis and performance of a large thermoacoustic engine // J. Acoust. Soc. Am. 1992, V.92, P.1551.
3. Gusev V., Bailliet H., Lotton P. and Bruneau M. Asymptotic theory of nonlinear waves in a thermoacoustic prime mover // Acust. Acta Acust. 2000, V.86, P.25.
4. Khokhlova V., Sapozhnikov O., Kascheeva S., Lotton P., Gusev V., and Job S. Effects of nonlinear saturation in propagation of acoustic waves in media with frequency dependent amplification // Sov. Phys. Izvestia Russ. Acad. Sci. 2001, V.64, P.2334.
5. Wakeland R.S. and Leolian R.M. Measurements of the resistance of parallel-plate heat exchangers to oscillating flow at high amplitudes // J. Acoust. Soc. Am. 2004, V.115, P.2071.
6. Yazaki T., Tominaga A. and Narahara Y. Large heat transport due to spontaneous gas oscillation induced in a tube with steep temperature gradients // Journ. Heat Transf. 1983, V. 105, P. 889-894.
7. Yazaki T. and Tominaga A., Measurement of sound generation in thermoacoustic oscillations // Proc. Roy. Soc. Lond. 1998, V. A 454, P. 2113-2122.
8. Menguy L. and Gilbert J., Nonlinear acoustic streaming accompanying a plane stationary wave in a guide // Acust. Acta Acust. 2000, V. 86, P. 249-259.
9. Thompson m. W. and Atchley A. A., Influences of a temperature gradient and fluid inertia on acoustic streaming in a standing wave // J. Ac. Soc. Am. 2005, V. 117, P. 1839.
10. Gusev V., Job S., Bailliet H., Lotton P. and Bruneau M., Acoustic streaming in annular thermoacoustic prime movers // J. Ac. Soc. Am. 2000, V. 108, P. 934.
11. Bailliet H., Gusev V., Raspet R., Hiller R.A., Acoustic streaming in closed thermoacoustic devices // J. Ac. Soc. Am. 2001, V. 110, P. 2678.
12. Penelet G, Job S, Gusev V, Lotton P. and Bruneau M., Dependence of sound amplification on temperature distribution in annular thermoacoustic engines // Acust. Acta Acust., 2005, V.91, P.567.
13. Penelet G., Gusev V., Lotton P. and Bruneau M., Experimental and theoretical study of processes leading to steady-state sound in annular thermoacoustic prime movers // to be published in Physical Review E, 2005.
14. Mac Adams W. H., Heat Transmission, 3rd ed., 1953.
15. Job S., Gusev V., Lotton P. and Bruneau M. Acoustic streaming measurements in annular thermoacoustic engines // J. Ac. Soc. Am. 2003, V. 113, P. 1892.
16. Rudenko O.V.; Solyyan S.I. Theoretical foundations of non-linear acoustics. Consultant Bureau, New York, 1978.